AD_____

Award Number:
W81XWH-11-1-0133

TITLE:
Characterizing SHP2 as a Novel Therapeutic Target in Breast Cancer

PRINCIPAL INVESTIGATOR:
Zachary Hartman

CONTRACTING ORGANIZATION:
West Virginia University
Morgantown, WV 26505

REPORT DATE:
April 2014

TYPE OF REPORT:
Annual Summary (Final)

PREPARED FOR: U.S. Army Medical Research and Materiel Command
Fort Detrick, Maryland 21702-5012

DISTRIBUTION STATEMENT:

x Approved for public release; distribution unlimited

The views, opinions and/or findings contained in this report are those of the author(s) and should not be construed as an official Department of the Army position, policy or decision unless so designated by other documentation.

REPORT DOCUMENTATION PAGE

Form Approved
OMB No. 0704-0188

1. REPORT DATE *(DD-MM-YYYY)*	2. REPORT TYPE	3. DATES COVERED *(From - To)*
April 2014	Annual Summary (Final)	15 JAN 2011 - 14 JAN 2014

4. TITLE AND SUBTITLE
Characterizing SHP2 as a Novel Therapeutic Target in Breast Cancer

5a. CONTRACT NUMBER

5b. GRANT NUMBER
W81XWH-11-1-0133

5c. PROGRAM ELEMENT NUMBER

6. AUTHOR(S)
Zachary Hartman

email: zhartma1@mix.wvu.edu

5d. PROJECT NUMBER

5e. TASK NUMBER

5f. WORK UNIT NUMBER

7. PERFORMING ORGANIZATION NAME(S) AND ADDRESS(ES)
West Virginia University

Morgantown, WV 26505

8. PERFORMING ORGANIZATION REPORT NUMBER

9. SPONSORING / MONITORING AGENCY NAME(S) AND ADDRESS(ES)
U.S. Army Medical Research and Materiel Command
Fort Detrick, Maryland 21702-

10. SPONSOR/MONITOR'S ACRONYM(S)

11. SPONSOR/MONITOR'S REPORT NUMBER(S)

12. DISTRIBUTION / AVAILABILITY STATEMENT

Approved for public release

13. SUPPLEMENTARY NOTES

14. ABSTRACT
During this research period, molecular modeling and biochemical studies were conducted to assess the roles of different acidic residues in the binding of the Src homology 2-containing protein tyrosine phosphatase (SHP2) to its substrates. A peptide derived from this substrate was shown to be a selective inhibitor of SHP2. SHP1 was used as a control, and the peptide did not act on this enzyme. Molecular modeling revealed key binding determinants at the atomic level present in SHP2 that could not be recapitulated in SHP1. These modeling observations were tested using mutation of the peptide. Indeed, when the peptide was mutated to abolish these interactions, inhibitory capacity was abolished entirely. Systematic mutation of the peptide *in silico* further demonstrated that the substrate needed to bind both of the positively-charged amino acid sidechains adjacent to the active site to facilitate the highest binding stability. Mutation of any of the acidic amino acids next to the phosphotyrosine on the substrate produced significant defects in binding as predicted by molecular docking. These findings are now being parlayed into study of the peptide-based inhibitor on cells, which is work that will continue into the coming year.

15. SUBJECT TERMS: nothing listed

16. SECURITY CLASSIFICATION OF:			17. LIMITATION OF ABSTRACT	18. NUMBER OF PAGES	19a. NAME OF RESPONSIBLE PERSON
a. REPORT	b. ABSTRACT	c. THIS PAGE			USAMRMC
U	U	U	UU	34	19b. TELEPHONE NUMBER *(include area code)*

Table of Contents

INTRODUCTION

The Src homology 2-containing protein tyrosine phosphatase (SHP2) is a positive regulator of cellular signaling and promotes breast cancer tumorigenesis. Because of this, it was hypothesized that SHP2 may be a useful therapeutic target in disease, since it acts as an integrator of numerous signaling pathways that are known to be dysregulated in cancer such as HER2. Previous cell biology work has demonstrated that SHP2 is required for maintenance of transformation. It has not been conclusively demonstrated that SHP2 would serve as an attractive therapeutic target. In addition, SHP2 inhibitors designed so far have failed to demonstrate selectivity over closely-related homologues such as SHP1 (1,2). This work was designed to first determine how SHP2 selectively binds its target substrates and then to apply this knowledge in the first-in-class demonstration of SHP2's viability as a therapeutic target in breast cancer.

Over the course of the three years of the fellowship period, research efforts have been focused on the statement of work tasks. The findings within each of the tasks completed will be presented here.

Task 1- Site-directed mutagenesis of HER2 and establishment of stable cell lines expressing the different HER2 proteins.

In order to determine the selectivity of SHP2 towards its substrates, we attempted a substrate-based approach. Our substrate-trapping mutant has previously been shown to form a selective interaction with phosphotyrosine 1023 of HER2. We wanted to know if mutation of the sequence surrounding this residue would abolish that interaction. To that end, we obtained the cDNA of HER2 and mutated the residues at positions 1021 and 1022. A double mutant was also obtained. The mutant cDNA was subcloned into a retroviral vector for viral packaging. Virus particles were obtained and used to infect MCF-10A cells, resulting in stable cell lines containing the E1021A, E1022A, or E1021/1022A mutants.

Task 2- Determine the binding specificity of SHP2 by substrate-trapping methods

Substrate trapping was performed using a purified, recombinant GST fusion of DM-SHP2, a catalytically-inactive yet binding-competent SHP2 mutant, incubated with total cell lysates containing HER2. All three mutants of HER2 failed to bind to SHP2 in this regard. We were especially interested in the E1021A mutant, however, since the negatively-charged amino acid located at this position is unique to substrates (see Figure 1A of the attached manuscript). We were able to demonstrate that the Y1023 still becomes phosphorylated via RasGAP co-immunoprecipitation, which measures an interaction that is phospho-Y1023-dependent.

In all, our experiments suggested that the sequence upstream of the substrate tyrosine is indeed critical for *in vivo* recognition of the full-length peptide.

Task 3- Synthesize and characterize anti-SHP2 peptides derived from the Y1023-HER2 in vitro

Tyrosine 1023 of HER2 becomes phosphorylated in response to different stimuli, including EGF. SHP2 is known to act upon this site, dephosphorylating it. Dephosphorylation prevents the binding of the signaling inhibitor RasGAP, resulting in enhanced signaling (3). Since this is the only site on HER2 known to be engaged by SHP2, it was hypothesized that a peptide derived from the substrate sequence could act as a selective inhibitor. Thus, the peptide sequence DADEpYL was synthesized (pY representing phosphotyrosine) and tested against SHP2 and SHP1 activity. The Cheng-Prusoff equation was used to convert the IC_{50} into the inhibitory constant, K_i. The results are reported in Table 1. This peptide was found to have a Ki against SHP2 of 11.92 micromolar, whereas in SHP1 the inhibitory constant was found to be 630 micromolar. This large selectivity for SHP2 is unprecedented in the design of small molecule inhibitors. Therefore, the substrate-derived peptide was shown to be significantly more selective for SHP2 compared to its close homolog, SHP1.

In line with the mutagenesis experiments, we synthesized a peptide corresponding to our E1021A mutant HER2, with the sequence DAAEpYL. This peptide was subjected to the same competitive inhibition assay against SHP2. As expected, the altered sequence resulted in very poor inhibition of SHP2.

Task 4- Molecular modeling of HER2 peptides

A preliminary analysis of the primary sequence of the two enzymes revealed some differences in the region surrounding the active site (Figure 1A). Specifically, lysine 364 (K364)

was found to be substituted with an arginine in SHP1, and arginine 362 (R362) of SHP2 was replaced by a lysine in SHP1. These residues have been previously suggested to play roles in selective binding of inhibitors(4). To understand how these differences may translate into conformational alteration of the active site, the crystal structures of SHP2 (2SHP.pdb) and SHP1 (1GWZ.pdb) were overlaid based on the catalytic region (Figure 1B). K364 in SHP2 was shown to be placed in the same location as an arginine in SHP1. These residues were conserved in terms of sidechain charge, but they differed significantly in terms of structure.

Since we found that the substrate-based peptide displayed selectively for inhibition of SHP2 activity over, we wished to identify the intermolecular interactions that might be critical for binding to both enzymes. Since no crystal structure of SHP2 bound to this phosphopeptide is available, we attempted to elucidate interactions with molecular docking (5). The peptide was docked into the SH2 active site of 2SHP.pdb (with SH2 domains stripped from the crystal) using the genetic algorithm. At least 2000 runs were performed, and the most favorable conformation was selected (Figure 2). We ensured that the phosphotyrosine was situated inside the active site near the catalytic cysteine, an essential characteristic of binding in the PTP mechanism(6). Electrostatic interactions were computed in Autodock Tools. Strong ionic contacts were found between arginines and lysines to the acidic residues of the substrate peptide (Table 2), with the most prominent being the -2 position aspartate residue to K364 (-6.737 kcal/mol). Other strong predicted interactions included two contacts with the -4 position aspartate of the peptide to arginine 362 (-2.827 and -3.653 kcal/mol). The -2 aspartate also interacted with lysine 366 (-0.113 kcal/mol). Finally, the -1 glutamate residue of the peptide was predicted to hydrogen bond with Y279 of SHP2 (-2.903 kcal/mol). The total intermolecular interaction energy was found to be -14.3 kcal/mol with -8.50 kcal/mol originating from Van der Waals interactions and hydrogen bonds and -5.80 kcal/mol provided by electrostatic interactions. Overall, the predicted Ki of the peptide was 9.72uM, which aligned reasonably well with the kinetics data we obtained.

Differences in selectivity for the peptide inhibitor were predicted by docking the same substrate-derived peptide into the SHP1 active site (Figure 3). Out of more than 2000 runs, the best docked structure predicted a Ki of 641 uM, a rather dramatic loss of predicted inhibition compared to SHP2. Analysis of the structure revealed many electrostatic contacts between the peptide and the active site (Table 2). Arginine 358, which is analogous to lysine 364 of SHP2, was predicted to form an ionic bond with the -2 position aspartate of the peptide (-4.518 kcal/mol) Another electrostatic interaction was found between histidine 420 and the -1 glutamate of the peptide (-3.67 kcal/mol). The geometry of the predicted interactions was influenced by steric clashes. The orientation and size of arginine 358 appeared to create a pocket that required deformation of the peptide and atom contacts with the active site, resulting in a lowered overall binding energy.

In order to further corroborate the docking calculations of the wildtype peptide, docking was used to perform an *in silico* alanine scan. This was done by mutating the peptide's acidic amino acids into alanine and predicting the new binding conformation and affinity of the molecule. In this way, three new peptides were assessed, mutating at the -4, -2, and -1 positions. The results of this experiment are reported in Table 3.

The -1 mutant peptide, DADApYL, demonstrated a significantly poorer predicted inhibition constant when compared to the wildtype peptide. The constant predicted for this peptide was found to be 493.5 μM. The predicted binding conformation of this peptide showed a tendency to form polar contacts with lysine 364 (Fig. 4). The peptide AADE predicted an even more pronounced loss of inhibition by the peptide, 608.21 μM. Both lysine 364 and 366 were targeted for interaction by the peptide (Fig. 5). Finally, the DAAEpYL peptide was docked, yielding a predicted inhibition constant of 611.38 μM. The most prominent sidechain interaction was found between lysine 364 and the -1 glutamate residue of the peptide (Fig. 6). This predicted inhibition is in reasonable agreement with the experimental results reported in Table 1 for this peptide.

The *in silico* alanine scan demonstrated two major findings about the binding of substrate peptide to SHP2. First, each of the acidic amino acids adjacent to the phosphotyrosine appears to play a critical role, since mutation of any of these engenders a dramatic loss of predicted binding capacity. Second, the peptides appear to show a preference for binding the lysine 364 residue to the exclusion of arginine 362 that was suggested to also play a deciding role in binding of the wildtype peptide. Since arginine 362 was not targeted, it

would appear that binding to this residue is a key constituent of strong binding that leads to the low micromolar affinity of the wildtype peptide. Both the lysine 364 and arginine 362 form strong interactions with the peptide. This is particularly compelling, because, as noted in Figure 1, these two residues are swapped in SHP1, and the wildtype peptide cannot dock and form the same interactions as strongly with the new residues.

When combined, these data present strong evidence that the driving force of SHP2 selectivity is the interaction of molecules with both the lysine 364 and arginine 362 residues adjacent to the active site. This information will prove valuable in the future design of inhibitors in this field, since to date no drug has been designed that specifically targets the lysine 364 and arginine 362.

Task 5- Test the efficacy of peptide inhibitors against SHP2-mediated cell signaling and transformation

The *in vitro and in silico* data of the peptide were compelling evidence for the substrate-derived peptide's ability to inhibit SHP2 activity in a selective manner. Next, it was determined what kind of effect this peptide might have on cells. As laid out in task 6 (Test the efficacy of peptide inhibitors against SHP2-mediated cell signaling and transformation), I tested the hypothesis that the peptide could act to inhibit SHP2 in cells, conferring an effect on signaling similar to that seen when SHP2 expression is inhibited using short-hairpin RNA. Specifically, suppression of SHP2 inhibits the ability for EGF to stimulate the mitogen-activated protein kinase (MAPK) pathway, which is read as a drop in phosphorylated ERK protein(3).

First, the problem of cell permeability needed to be overcome. The phosphobenzene moiety of the peptide confers significant negative charge to the peptide, making it unlikely to enter the cell spontaneously. To solve this problem, the peptide sequence was altered to include the cell-penetrating sequence from the HIV TAT1 protein, which has been shown to facilitate delivery of different types of cargo into cells (7). The peptide was also tagged with fluorescein isothiocyanate (FITC) to determine if it was being successfully internalized into cells. BT474 has been tested so far with this peptide. These HER2-positive cancer cells are ideal to model EGF response and dependence on SHP2. First, they were grown to confluence. Once they reached this stage, the cells were serum-starved overnight. The following morning, the peptide was incubated with the cells for one hour before EGF was added to a concentration of 100 ng/mL. The FITC channel of an Olympus X78 microscope was used to verify internalization of the FITC tag (Figure 7). It was noted that the phosphorylated form of the peptide was able to localize to the membrane in response to EGF, which suggests that it may be acting upon SHP2 in this region. SHP2 is recruited to the membrane independently of HER2 through the Grb2-associated protein 2, an adapter molecule that is recruited to the membrane following EGF stimulation. The non-phosphorylated peptide did not show this same localization, but it was significantly internalized thanks to the TAT1 tag.

Under the same conditions, EGF-mediated activation of the MAPK signaling pathway was tested in the presence of the phosphorylated and non-phosphorylated peptides (Figure 8). The non-phosphorylated peptide showed no change in the signaling intensity or duration, while the phosphorylated form strongly inhibited both the initial spike and the duration of phosphorylated ERK signal. These results strongly suggest that the substrate-derived peptide inhibitor can suppress SHP2 activity in cells in addition to *in vitro* experiments.

In the coming months, this peptide will be tested in other cell lines and against other phenotypes related to cancer. These include migration and anchorage-independent growth.

OTHER ACCOMPLISHMENTS NOT ASSOCIATED WITH TASKS

Our 2009 paper establishing HER2 as an important target for SHP2 activity was a landmark in the role of SHP2 in breast cancer biology. Unfortunately, this paper left a few questions unanswered regarding the mechanism by which SHP2 promotes HER2-mediated signaling. For example, dephosphorylation of the RasGAP binding site Y1023 was clearly important, but other labs have established different roles for SHP2 in promoting Ras-mediated signaling downstream of HER2.

Our mutagenesis of the sequence upstream of Y1023 gave us a unique platform to decouple the binding of RasGAP and the binding of SHP2, a feat previously not demonstrated. We reasoned that if SHP2 were

principally needed to dephosphorylate Y1023, then the transformative capacity of the E1021A mutant should be hindered compared with wildtype HER2. Thus, we subjected the MCF-10A cells stably expressing the mutant or wildtype HER2 proteins to EGF stimulation and soft agar anchorage-independent growth assays (see Figure 3 of the attached manuscript). Interestingly, in both experiments, mutation of HER2 that abolishes SHP2 binding results in enhanced signaling compared with empty vector control cells, but the transformation is not as robust as in cells expressing the wildtype HER2 protein.

KEY RESEARCH ACCOMPLISHMENTS

- A peptide derived from the known SHP2 substrate HER2 is a selective inhibitor of enzymatic activity *in vitro*.
- The -2 position acidic amino acid of the substrate is critical for binding both *in vitro* and *in vivo*.
- Association with positively charged amino acids lysine 364 and arginine 362 is critical for binding SHP2.
- The same binding interactions for SHP2 cannot be recapitulated in SHP1 despite similarities in sequence. The structure of the active site of SHP1 does not allow for the same interactions to occur.
- The substrate-derived peptide, once fused to a cell-penetrating sequence, can act as an inhibitor of SHP2-mediated signaling in HER2-positive breast cancer cells.

REPORTABLE OUTCOMES

- Poster presentation at the 2013 WVU Van Liere Research Day
- Final stages of paper submission to the Journal of Biological Chemistry regarding the mechanism of SHP2 selectivity

CONCLUSIONS

The work gathered into this report represents a significant milestone in the characterization of SHP2. To date, many labs have attempted to design or screen for inhibitors against this enzyme with little success (2,4,8-10). This work has yielded some very interesting observations regarding what can make for a selective inhibitor, but no group has yet reached satisfactory levels. What the results presented here show is that selectivity can be achieved for SHP2 over SHP1 (the most challenging enzyme pair to inhibit selectively due to sequence homology), and, more importantly, it is the association of negatively-charged functional groups with the positively-charged amino acids of SHP2 adjacent to the active site that mediate the selectivity. Specifically, interactions with both arginine 362 and lysine 364 near the active site appear to be crucial for binding to SHP2, since mutations in the peptide that abolish one of these interactions remove the inhibitory capacity. These same interactions cannot be formed by the peptide in SHP1 as predicted by molecular docking, suggesting a strategy for selective inhibition by a peptidomimetic.

In addition, our work has provided a better understanding into the mechanism of SHP2 promotion of HER2-mediated signaling and transformation.

Note Regarding Task 7

Unfortunately, the long-term experiments using cells and mice in the presence of the substrate-derived peptide inhibitor proved prohibitively challenging to complete. We encountered two principal problems with their application. First, the phosphotyrosine moiety has a very low half-life in the presence of cells. In our experience, any inhibitory effects conferred by adding phosphotyrosine-containing peptides to cells lasted a few hours, at most. This precluded study in long-term anchorage-independence assays and mouse studies. In addition, peptides in general are not known to be bioavailable.

We feel the importance of this work rests on two principles. One, the molecular modeling is a first-in-class portrait of atomic interactions that contribute to selective binding. These findings should contribute to the development of a selective inhibitor, an ongoing project with some initial success that we are currently seeking patent protection for. Second, we were able to provide a better basis for the promotion of signaling by SHP2 in a unique way. Mutagenesis of phosphatase substrates upstream of the substrate phosphotyrosine itself is an approach not often taken in this field. By uncoupling phosphatase activity from most normal function of the residue, we were able to clearly show how important binding of SHP2 to Y1023 is. These findings further support the rationale for targeting SHP2 in breast cancer.

TRAINING ACCOMPLISHMENTS

Courses

BMS 705 Cellular Structure and Metabolism
BMS 710 Fundamentals of Integrated Systems
BMS 715 Molecular Genetics
BMS 734 Cell Signaling and Metabolism
BMS 720 Scientific Writing
CHEM 531 Advanced Organic Chemistry I
BIOC 750 Protein Chemistry/Enzymology
CCB 705 Basic/Clinical Aspects of Cancer
Associated Biochemistry and Cancer Cell Biology Journal Clubs

Molecular Biology Skills Obtained

Western blotting
Cell culture
Site-directed mutagenesis
PCR
Subcloning
Protein purification
Immunoprecipitations
Affinity Precipitations
Immunofluorescence
Anchorage-independence assays
Wound healing assays
Live-cell imaging
Mouse xenografts
Enzymatic activity assays
Cell viability studies

Symposia attended

San Antonio Breast Cancer Symposium 2011
San Antonio Breast Cancer Symposium 2012
American Association for Cancer Research 2013

Society Memberships

American Association for Cancer Research, 2013-present

Publications

Submitted Hartman ZR, Agazie YM. Substrate discrimination by the Src homology 2-containing protein tyrosine phosphatase SHP2 predicted by molecular docking

Hartman ZR, Schaller MD, Agazie YM. The tyrosine phosphatase SHP2 regulates focal adhesion kinase to promote EGF-induced lamellipodia persistence and cell migration.

Hartman Z, Zhao H, Agazie YM. HER2 stabilizes EGFR and itself by altering autophosphorylation patterns in a manner that overcomes regulatory mechanisms and promotes proliferative and transformation signaling.

SUPPORTING DATA

Table 1. Inhibition of SHP1 and SHP2 by substrate-derived peptides.

Peptide	Predicted Ki (μM)	Experimental Ki (μM)
DADEpYL		
SHP1	641	630.0
SHP2	9.72	11.97
DAAEpYL		
SHP2	611.38	856.8

Table 2. Predicted electrostatic energies of interactions between the peptide and SHP1/SHP2[a]

Peptide to SHP2	Energy	Peptide to SHP1	Energy
-1 Glu to Y279	-2.903	-1 Glu to H420	-3.67
-2 Asp toK364	-6.737	-1 Asp to K356	-0.301
-2 Asp to K364	-0.113	-2 Asp to R359	-4.518
-4 Asp to R362	-2.827	-2 Asp to R359	-0.26
-4 Asp to R362	-3.653	-4 Asp to K356	-0.007

[a] Energy in kcal/mol

Table 3. *In silico* alanine scan of the peptide, bound to SHP2

Peptide	Predicted Ki (μM)
DADApYL	493.5
DAAEpYL	611.38
AADEpYL	608.21

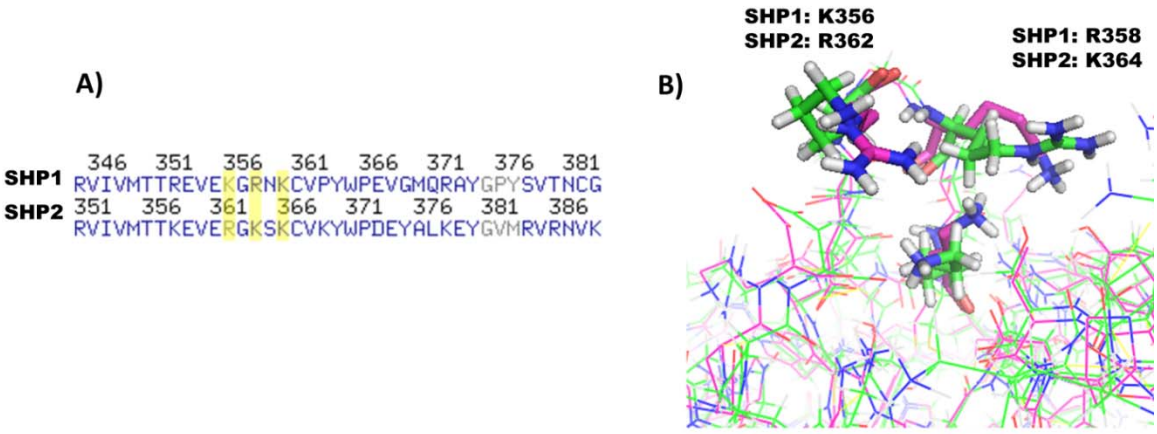

Figure 2. Comparison of the SHP1/SHP2 active sites
a) Overlay of the primary sequence of the non-conserved active site regions between SHP1 and SHP2 b) Overlay of the SHP1 (1GWZ.pdb) and SHP2 (2SHP.pdb) active sites. SHP1 backbone is colored in green, and SHP2 is colored pink. The highlighted residues from A are presented as licorice models, and the conserved active site arginine and cysteine residues are highlighted for reference.

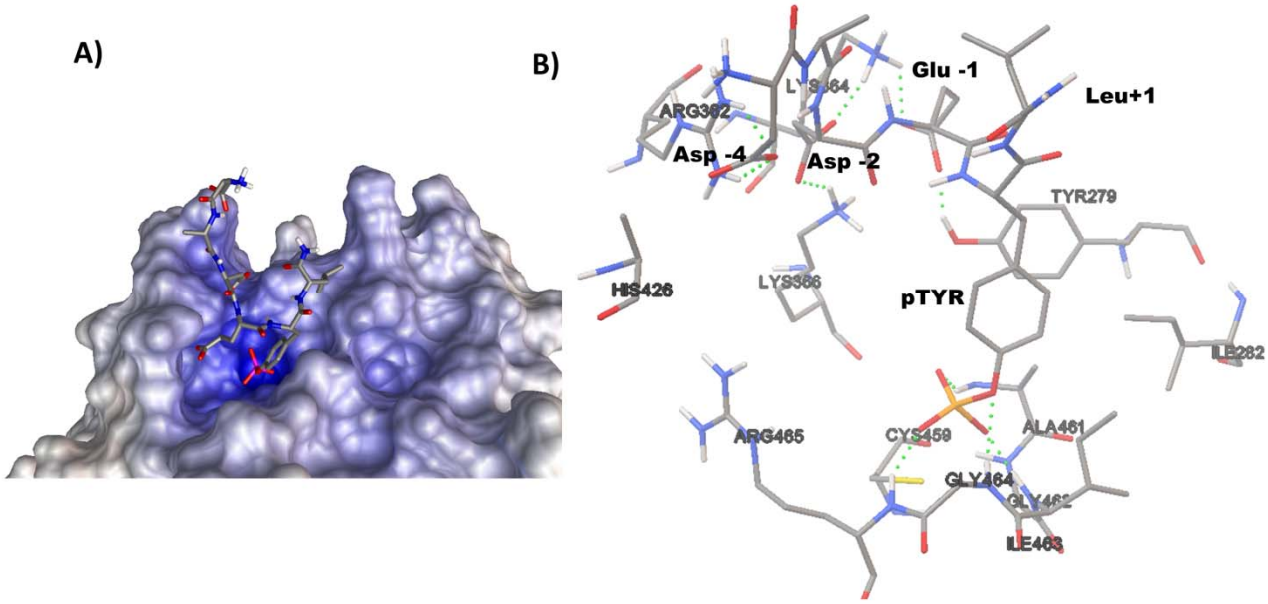

Figure 1. Computational docking of the substrate-derived peptide into the SHP2 active site
a) EGFR Y992-derived peptide was docked into the SHP2 active site using Autodock4, and the binding mode is presented with SHP2 residues represented using the CPK model. b) Interactions between the peptide and the SHP2 active sites. Peptide residues are labeled based on their sequence position relative to the phosphotyrosine. Polar contacts are indicated by green dots.

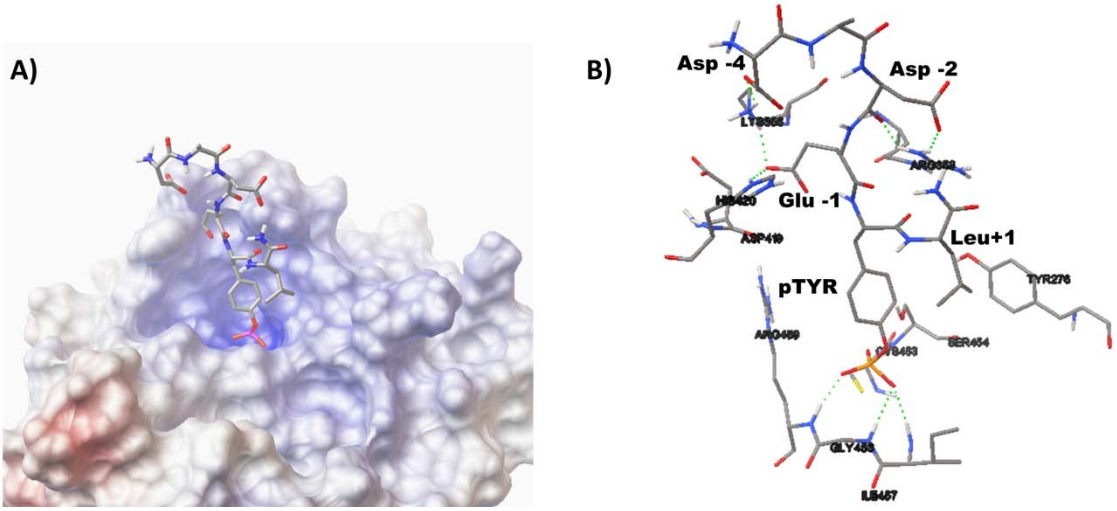

Figure 3. Computational docking of the substrate-derived peptide into the SHP1 active site
a) Substrate-derived peptide was docked into the SHP1 active site using Autodock4, and the binding mode is presented with SHP1 residues represented using the CPK model. b) Interactions between the peptide and the SHP1 active sites. Peptide residues are labeled based on their sequence position relative to the phosphotyrosine. Polar contacts are indicated by green dots.

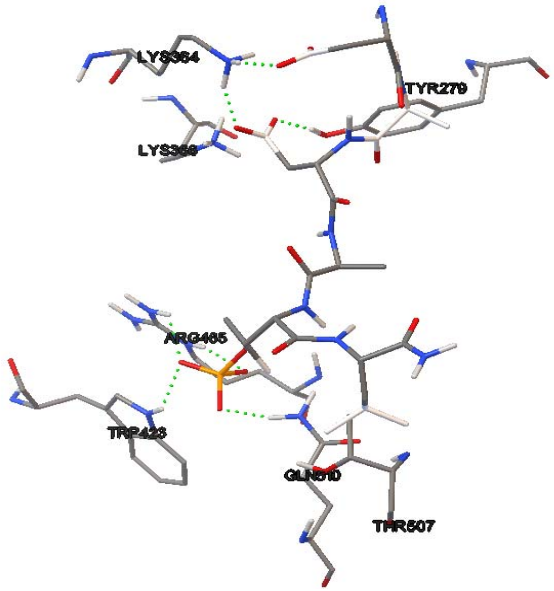

Figure 4. Predicted binding conformation of the DADApYL peptide to SHP2. Predicted hydrogen bonds are represented by green spheres.

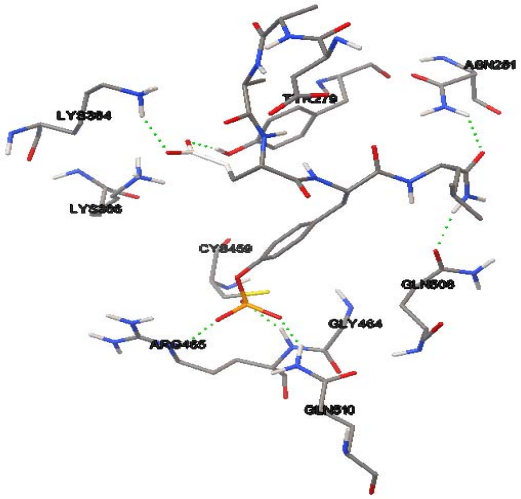

Figure 5. Predicted binding conformation of the DAAEpYL peptide to SHP2. Predicted hydrogen bonds are represented by green spheres.

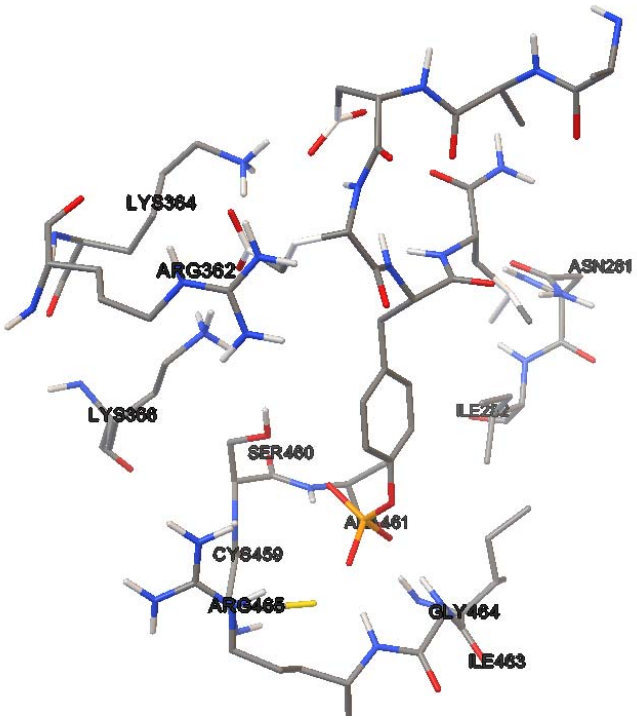

Figure 6. Predicted binding conformation of the AADEpYL peptide to SHP2. Predicted hydrogen bonds are represented by green spheres.

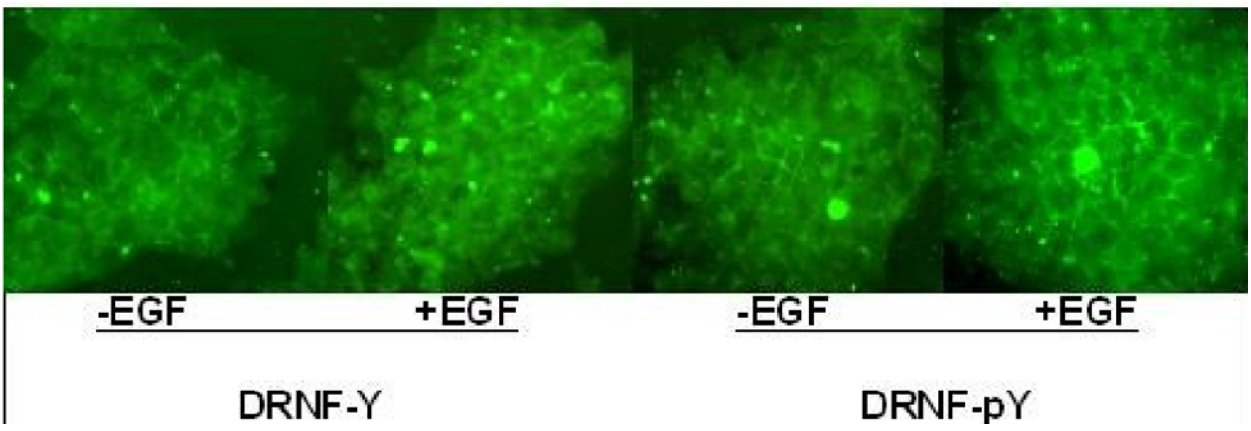

Figure 7. Successful internalization and pY-dependent membrane localization of the FITC-tagged substrate-derived peptide. BT474 cells were grown to confluence before serum-starving overnight. Then, EGF (100 ng/mL) was added in the presence of either phosphorylated peptide or non-phosphorylated peptide. Penetration into the cell was facilitated by incorporating the cell-penetrating peptide sequence from HIV-TAT1.

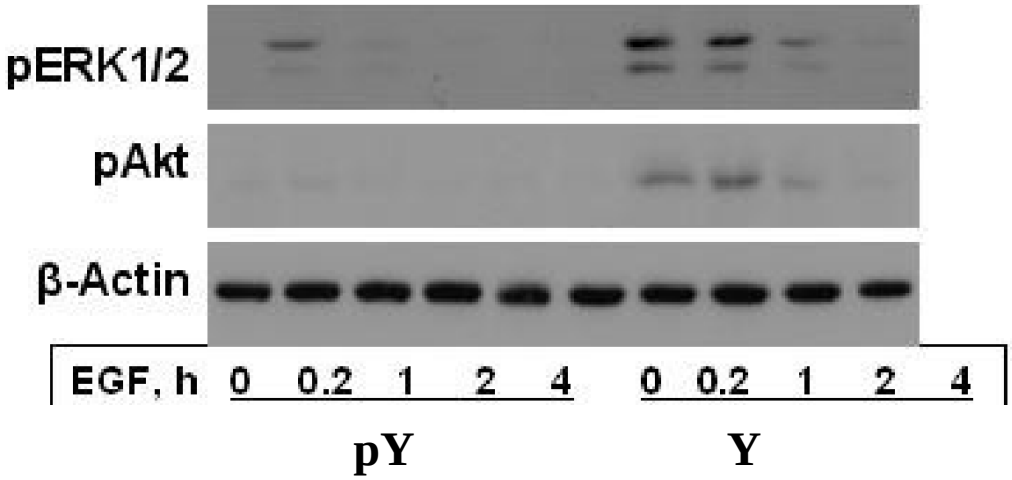

Figure 8. A phosphorylated substrate-based peptide acts as an inhibitor of signaling *in vitro*. BT474 cells were grown to confluence before serum-starving overnight. Then, EGF (100 ng/mL) was added for the indicated times in the presence of either phosphorylated peptide or non-phosphorylated peptide. Penetration into the cell was facilitated by incorporating the cell-penetrating peptide sequence from HIV-TAT1.

APPENDED MANUSCRIPT: SUBSTRATE DISCRIMINATION BY THE SRC HOMOLOGY 2-CONTAINING PROTEIN TYROSINE PHOSPHATASE SHP2 PREDICTED BY MOLECULAR DOCKING

Abstract

The tyrosine phosphatase SHP2 is a positive regulator of mitogenic and cell survival signaling. In the signaling of receptor tyrosine kinases, especially EGFR and HER2, SHP2 is known to act on binding sites for RasGAP. However, it is not clear exactly how SHP2 recognizes these sequences selectively. In this report, a substrate-based peptide is shown to be a selective inhibitor for SHP2 over its homologue SHP1. The proto-oncogene HER2 was expressed in MCF-10A cells, and a mutation upstream of the phosphotyrosine 1023 abolished association with the SHP2 active site. This dissociation of the SHP2-HER2 interaction correlated with impaired EGF-induced signaling and transformation normally induced by HER2. Computational docking of the substrate-derived peptide identified SHP2 arginine 362 and lysine 364 as key mediators of binding. These data suggest key substrate-protein interactions that allow for selective binding.

Introduction

The Src homology 2-containing protein tyrosine phosphatase 2 (SHP2) is a cytosolic PTP that mediates many important signaling networks (6). It contains two tandemly-arranged SH2 domains that generate intramolecular autoinhibition of the catalytic active site. Binding to phosphotyrosine induces a conformational change that relieves this inhibition (11). When active, SHP2 functions to promote signaling related to proliferation (12), survival (13,14), and motility (15). This positive functionality of SHP2 is critical for promotion of different forms of cancer (16). In cells, SHP2 is required for maintenance of the transformed phenotype of fibroblasts expressing an oncogene (17). It is also required to promote the mesenchymal state and anchorage-independent survival in breast cancer cell lines (18). Thus, targeting SHP2 with small molecules appears to be an attractive means of combating cancer, but development of these inhibitors has proved challenging.

To date, numerous studies have been published characterizing inhibitors based on high-throughput chemical and *in silico* drug screens (1,4,9,10,19). A few common challenges have appeared through this work. First, moieties used to mimic phosphotyrosine tend to be charged, rendering the compound impermeable to the cell membrane. Selectivity of these compounds is another significant issue. The active sites of PTPs are well-conserved in sequence and overall charge distribution (20). Thus, many drugs that target SHP2 tend to target

other PTPs, especially its homolog SHP1. This is an especially-important issue to overcome since SHP1 is a negative mediator of signaling (21). The most selective inhibitors for SHP2 have been shown to achieve approximately 20-fold selectivity for SHP2 over SHP1 (4), which leaves significant room for improvement. SHP2 is known to selectively bind substrates *in vitro (22)*. This observation suggests that the issue of drug selectivity can be surmounted. Unfortunately, the intermolecular determinants of selective substrate binding to SHP2 have not been elucidated. A study exploring the peptide sequence best-recognized by SHP2 has been published (23). The specific molecular interactions required for selective binding remain to be elucidated, however. Numerous crystal structures of unbound (11) and small molecule inhibitor-bound SHP2 (9) have been published, but to date no study has been undertaken to elucidate the molecular determinants of a substrate binding to SHP2. To this end we have performed docking experiments along with biochemical validation to test how a substrate-based inhibitory peptide is able to selectively inhibit SHP2 over SHP1. The results presented herein suggest the presence of key electrostatic and steric interactions that allow the peptide to bind SHP2 but not SHP1 and help pave the way toward selective SHP2 inhibitor design.

Materials and Methods

Cells, cell culture, and reagents

The immortalized mammary epithelial cell line MCF-10A were purchased from American Tissue Culture Collection (ATCC). These cells were cultured in Dulbecco's modified Eagle's medium supplemented with 10 μg/ml recombinant human insulin, 20 ng/ml EGF (PeproTech), 0.5 μg/ml hydrocortisone, 100 ng/ml cholera toxin (Sigma), and 5% horse serum. Other reagents used included the DiFMUP kit (Invitrogen) and glutathione-sepharose beads (GE Healthcare); peptides corresponding to the SHP2 target site of EGFR (DADEpYL) were synthesized and purified to greater than or equal to 95% by NeoPeptide, Inc.

The anti-HER2 antibody was from Sigma. Anti-phospho-ERK 1/2 and phospho-Akt were from Cell Signaling, Inc. The anti-RasGAP antibody was from BD Biosciences.

Purification of recombinant GST fusion proteins

The method used for expressing and purifying the GST fusion of the PTP domain of SHP1 and SHP2 has been described previously (24). To summarize, E. coli expressing the plasmid pGEX with either SHP2 or SHP1 were grown overnight in 100 mL luria bertani (LB) broth. Then the culture was diluted 1:5 with LB and was stimulated with 1 mM IPTG for approximately 3 h. The bacteria were harvested by centrifugation before lysis

in a buffer containing 20 mM HEPES, 120 mM NaCl, 10% glycerol, 0.5% NP-40, and 2 mM EDTA. Sonication was used to assist the lysis, and then the lysate was incubated for 30 minutes with Triton X-100 before being cleared by centrifugation. The supernatant was applied to a slurry of glutathione sepharose beads overnight at 4°C. The beads were washed with lysis buffer three times, and the protein was eluted using reduced glutathione (10 mM) in tris buffer. The eluted product was collected and stored in -80oC with 10mM dithiothreitol. The Bradford assay (Biorad, City, State) was used to quantify the product.

In vitro phosphatase activity assay

Purified SHP2 or SHP1 lacking the regulatory SH2 domains was diluted to a concentration of 5 nM with phosphatase reaction buffer (50mM HEPES, 100 mM NaCl, and 2 mM EDTA, pH=7.2). Difluoromethylumbelliferryl phosphate was used as an artificial substrate at a concentration of 20 uM or 35 uM, corresponding to the Km for SHP2 and SHP1, respectively. Varying concentrations of peptide (sequence DADEpYL corresponding to the substrate phospho-Y992 of EGFR) were used to assess which concentration resulted in 50% inhibition. Graphpad Prism 5 was used to calculate this IC50 value. Ki was calculated based on the Cheng-Prusoff equation:

IC50=Ki(1+[S]/Km)

Site-directed mutagenesis, subcloning, and expression of HER2

HER2 cDNA in a pCMV-SPORT6 vector, purchased from ATCC, was used as the template for site-directed mutagenesis using a Stratagene kit (600250). The sense and the antisense primers for the E1021A substitution were 5'-GGACCTGGTGGATGCTGCGGAGTATCTGGTACCCCAGCAG-3' and 5'-CTGCTGGGGTACCAGATACTCCGCAGCATCCACCAGGTCC-3'. Both the wildtype and mutant cDNAs were then ligated into the REBNA/IRES/GFP viral vector reported previously at XhoI and NotI sites using the forward primer containing a SalI site (5'-TTTGTCGACCGCCACCATCGCAGCT-3') and a reverse primer containing a NotI site (5'-TTTTGCGGCCGCCTATTTATCATCATCAT-3') (24). Retroviruses were generated, and MCF-10A cells were infected to stably express the wildtype and HER2 mutant as described previously using blasticidine selection (1 μg/mL) (24).

Preparation of cell lysates, immunoprecipitation, and immunostaining

Cells were lysed in a buffer containing 20 mM Tris–HCl (pH 7.4), 150 mM NaCl, 1 mM EDTA, 1% Triton-X-100, 10% glycerol, and 50 mM NaF supplemented with 10 μg/mL each of aprotinin, leupeptin, and

phenylmethylsulfonylfluoride (PMSF) for inhibition of proteases, and 10 mM sodium orthovanadate for inhibition of phosphatases. For immunoprecipitation, the lysates were cleared by centrifugation at 12,000 rpm, incubated overnight with a primary antibody, and then precipitated using protein G sepharose beads. The beads were washed 3 times with cell lysis buffer and denatured by boiling with Laemmli sample buffer. The same denaturation procedure was used for analyzing total cell lysates. Denatured proteins were separated on 8% or 10% PAGE, immobilized onto a nitrocellulose membrane, blocked with 3% bovine serum albumin (BSA) in tris-buffered saline containing 1% Tween-20 (TBST), and stained with a primary antibody overnight at 4°C. Next, membranes were washed three times with TBST, incubated with horseradish peroxidase–conjugated secondary antibodies in 5% milk, washed three times with TBST, and visualized by the chemiluminescence method (Pierce Inc.).

Affinity precipitation

The GST fusion of the PTP domain of doubly-mutated SHP2 (D425A and C459S, DM-SHP2) was used to affinity precipitate the wildtype and mutant HER2 as described previously (24). Briefly, cells at 80% confluence were incubated with 1 mM vanadate for 30 minutes before stimulating with EGF (100 ng/mL) for 10 minutes. Lysates were then incubated with purified GST-DM-SHP2 overnight at +4°C, and the resulting SHP2-substrate complexes were captured by incubating the mixture with glutathione sepharose beads for two hours at +4°C. The beads were then washed four times with lysis buffer before adding laemmli sample buffer and boiling. The denatured samples were then subjected to separation by SDS-PAGE and analysis by immunostaining.

Anchorage-independent growth assay

The soft agar assay was performed as described previously (25). Briefly, 6 cm cell culture plates were coated with 0.5% agar in growth medium. Approximately $1x10^5$ cells were suspended in growth medium that was mixed with melted agar to a final concentration of 0.5% and were then poured onto the agar bed. After four weeks of incubation a minimum of 10 fields at a 4x objective per plate were analyzed. Phase contrast pictures were taken using an Olympus IX71 microscope equipped with Olympus DP30BW digital camera, and colony size was estimated as a circular area using the measurement tools in Microsuite Basic Edition. Error bars represent the standard error of mean (SEM) of replicates.

Molecular docking

was built in InsightII (Accelrys, Inc.) and saved as a pdb. The docking pre-processing and data analysis were performed in Autodock Tools (26) and the grid and docking calculations were carried out by Autogrid4 and Autodock4 (5). Nonpolar hydrogens were removed from the peptide, and Kollman charges were added. The relaxed enzyme pdb was then loaded, and an 80x80x80 grid box with 0.375 angstrom grid spacing was placed around the point defined by the sulfur of the catalytic cysteine offset in the x direction by 16 angstroms. Electrostatic maps for the ligand were calculated based on this grid, and then the genetic algorithm was applied to search for the best predicted binding structure of the peptide. In each case a minimum of 2000 runs were attempted. Default parameters were used for the genetic algorithm with a few exceptions. First, population size was increased to 400, and the number of energy evaluations was set at a high number to allow for the maximum number of generations, which was set at 27000. Autodock Tools was then used to identify the best predicted binding pose, and pictures and hydrogen bonding information were gathered.

Results

A substrate-derived peptide is a selective SHP2 inhibitor

Previous reports showing discrimination by SHP2 of specific phosphotyrosine sites within the same protein (i.e., EGFR (27), HER2 (24), and FAK (28)) suggest that selectivity for substrates can be mediated by elements of the sequence surrounding the phosphotyrosine, as has been examined using library methods (29). Interestingly, when the primary sequences of the substrate and non-substrate phosphotyrosines were aligned, the presence of acidic amino acids seemed to be the most common trend. This was especially noted for the -2 position, which is the only residue where the acidic amino acid is fully conserved and exclusive to substrates (Figure 1A).

These observations led us to speculate that a phosphopeptide derived from the substrate sequence may act as a competitor to phosphatase activity. Since the endogenous substrate is thought to be selective for SHP2 as opposed to SHP1 (30,31), we hypothesized that the competition using this molecule would be similarly selective. A hexapeptide was synthesized to include the four amino acids N-terminal to the phosphotyrosine, since this region contained the highest amount of conserved acidic amino acids. The GST fusion of the PTP domains of SHP2 and SHP1 were purified as described in the materials and methods and used for in vitro phosphatase assays (32). The enzymatic activity of SHP2 and SHP1 toward the artificial

substrate difluoromethylumbelliferryl phosphate (DiFMUP) was determined in the presence of different peptide concentrations. We determined the inhibitory constant, Ki, for the peptide against both enzymes, resulting in more competition for SHP2 compared with SHP1 (approximately 11.97 μM SHP2 vs 630.0 μM for SHP1) (Figure 1B). These data support the hypothesis that a substrate-derived inhibitor of SHP2 does not readily inhibit SHP1, and selectivity for this inhibitor is based on the amino acids surrounding the phosphotyrosine.

Since the acidic amino acid located at the -2 position in the substrate sequence was well-conserved and exclusive to substrate phosphotyrosine sequences (Figure 1A), a modified peptide was synthesized substituting the -2 position aspartate for alanine, removing the associated negative charge. This substitution effectively eliminated the inhibitory ability of the peptide when subjected to phosphatase assays against SHP2 (Ki = 856.8 μM, Figure 1B). These results suggest that the conserved -2 position amino acid of the substrate is especially important for binding to SHP2.

Mutation of HER2 abolishes interaction with SHP2

Intracellular association of SHP2 with its substrates has been well established using the substrate-trapping, phosphatase-dead SHP2 mutant (DM-SHP2) (24,27,33). Since we observed that mutation in the substrate-derived peptide sequence was able to abrogate inhibition of the enzyme, we wanted to assess whether similar mutations in a full-length substrate could prevent its association with SHP2.

Using site-directed mutagenesis, we introduced an aspartate-to-alanine substitution in the HER2 protein at position 1021, corresponding to the -2 position aspartate in the substrate-derived peptide. Using a retroviral vector, the mutant or wildtype HER2 was expressed in the immortalized non-transformed breast epithelial cell line MCF-10A. Next, the cells were grown to near confluence before overnight starvation followed by vanadate treatment and EGF stimulation to enhance phosphorylation of HER2. Lysates were incubated overnight with a GST fusion of the DM-SHP2 PTP domain, and the resulting complexes were captured using glutathione sepharose beads. Wildtype HER2 was able to bind SHP2 in this context, whereas the Y1023F mutant HER2 was unable to form a complex with SHP2, as described previously (24). However, the D1021A mutant HER2 was unable to form a complex with SHP2 (Figure 2A). This suggested either the D1021A mutant of HER2 was poorly phosphorylated due to altered recognition by a kinase domain, or the mutation abolished the binding capacity for SHP2.

Antibodies selective for phosphorylated Y1023 have yet to be developed, so direct testing of the phosphorylation status of this residue would prove challenging. It has been demonstrated, however, that

phosphotyrosine 1023 acts as a major docking site for the SH2 domain of p120 RasGAP (24), and if the phosphorylation status is intact, binding to RasGAP should be preserved. To this end, we immunoprecipitated RasGAP out of EGF-stimulated MCF-10A cells expressing the HER2 proteins and probed for HER2 (Figure 2B). Both the wildtype and D1021A HER2 immunoprecipitated with RasGAP, while the Y1023F mutant did not to a significant extent. This suggests that the phosphorylation of D1021A HER2 at Y1023 was unaffected by the amino acid substitution, leading to the conclusion that the defective association with SHP2 is due to the removal of the acidic amino acid N-terminal to the phosphotyrosine.

Disruption of HER2-SHP2 interaction reduces transformation by HER2

It has been suggested that wildtype SHP2 promotes mitogenic signaling through HER2 by dephosphorylating tyrosine 1023 and preventing the association of RasGAP (24). We sought to determine the consequence of disrupting the SHP2-HER2 interaction while leaving the HER2-RasGAP interaction in place. To test this, we assessed EGF-induced signaling in cells expressing wildtype and D1021A HER2. Overexpression of wildtype HER2 resulted in prolonged Ras/MAPK and Akt signaling compared with control cells (24) (Figure 3A). However, when D1021A HER2 is overexpressed instead, the signal was still prolonged compared with controls, but it was not as robust as in cells overexpressing the wildtype HER2.

If the MAPK and Akt signaling cascades downstream of the HER2-SHP2 interaction were disrupted by mutation of HER2, then it should be expected that transformation by HER2 would be affected, as well. HER2 has been previously shown to promote transformation of MCF-10A cells as assessed by the soft agar assay, a measure of anchorage-independent growth (24). Therefore, we determined the effect of overexpressing mutant HER2 on formation of colonies in soft agar. As expected, wildtype HER2 formed significantly larger colonies compared with controls. However, when the D1021A mutant was overexpressed, the colonies were nearly 50% smaller on average compared with WT HER2-overexpressing cells (Figure 3B). These colonies were significantly larger than control, suggesting that the mutant HER2 maintained partial transformative capability. These observations in soft agar corresponded with those seen in the EGF-induced signaling cascades, where D1021A attenuated but did not eliminate the advantage conferred by overexpressing wildtype HER2 (Figure 3A). It should be noted that the MCF-10A cells are grown in cell media specifically supplemented with EGF, and this media was changed once every two days. Overall, these results support the hypothesis that SHP2 promotes HER2 signaling by dephosphorylating pY1023 following EGF stimulation, preventing recruitment of RasGAP and subsequent attenuation of the MAPK signaling cascade.

Molecular modeling predicts binding determinants of SHP2 and substrate

The results described so far suggested that binding of substrate by SHP2 is supported by negatively-charged amino acids upstream of the phosphotyrosine. Indeed, the region surrounding the active site of SHP2 is highly-positively charged, moreso in general than its homologue SHP1 (34). In order to assess how the substrate-based peptide binds to SHP2 selectively, we performed molecular docking studies using Autodock to predict binding of the peptide used in Figure 1 to the SHP1 and SHP2 active sites. The DADEpYL peptide was docked into the SHP2 active site of 2SHP.pdb (with SH2 domains stripped from the structure) using the genetic algorithm. At least 2000 runs were performed, and the most favorable conformation was selected to predict the interaction (Figure 4). We ensured that the phosphotyrosine was situated inside the active site near the nucleophilic cysteine, an essential step of the PTP catalytic mechanism (35). In these data, actual amino acid numbers in the SHP2 protein were used to refer to residues in the active site, while the position in reference to the pY was used to assign numbers to the residues in the peptide. Accordingly, residues N-terminal to the pY were assigned with negative numbers while those positioned C-terminal to the pY were given positive numbers.

Electrostatic interactions were computed in Autodock tools to estimate binding energies. Strong ionic contacts were found between arginine (R) and lysine (K) residues of the SHP2 active site and the acidic residues of the substrate peptide (Table 1), with the most prominent being between K364 and the aspartate residue at the -2 position (-6.737 kcal/mol). Other strong predicted interactions included two contacts between R362 and the aspartate in the -4 position of the peptide (-2.827 and -3.653 kcal/mol). The -2 aspartate also interacted with K366 (-0.113 kcal/mol). Finally, the -1 glutamate residue of the peptide was predicted to hydrogen bond with Y279 of SHP2 (-2.903 kcal/mol). The total intermolecular interaction energy was found to be -14.3 kcal/mol with -8.50 kcal/mol originating from Van der Waals interactions and hydrogen bonds and -5.80 kcal/mol provided by electrostatic interactions. We also calculated the predicted Ki of the peptide, which was found to be 9.72 μM.

To obtain further insight into the active site differences, the same peptide was docked into the SHP1 active site (Figure 5). Out of more than 2000 runs, the best structure predicted a Ki of 641 μM, a rather dramatic loss of predicted inhibition compared to SHP2 (9.72 μM). Analysis of the structure revealed many electrostatic contacts between the peptide and the active site (Table 2). R358, which is analogous to K364 of SHP2, was predicted to form an ionic bond with the -2 position aspartate of the peptide (-4.518 kcal/mol). Another electrostatic interaction was found between H420 and the -1 glutamate of the peptide (-3.67 kcal/mol). The geometry of the predicted interactions was influenced by steric clashes. The orientation and

size of R358 appeared to create a pocket that required deformation of the peptide and atom contacts with the active site, resulting in a lowered overall binding energy.

Discussion

This work demonstrates for the first time that a PTP substrate-based inhibitor can act as a selective antagonist of SHP2 activity compared to SHP1, a closely-related PTP family member. Here we have shown that critical interactions occur between active site basic residues and acidic residues of the peptide substrate.

Our initial observation that the substrate-derived peptide acted as a selective antagonist of SHP2 activity led to the idea that negatively-charged sidechains must play a critical role in SHP2 recognition of substrates, an idea that has been suggested by numerous studies (9,10,23,36). We have demonstrated for the first time, however, the critical importance of acidic amino acids to binding, since removal of even one of these residues (the -2 position aspartate) abolishes competition for substrate in the *in vitro* experiments (Figure 1B). We took this observation one step further, expressing the substitution in a cellular context with a *bona fide* SHP2 substrate, HER2. This mutant HER2 failed to associate with SHP2 via affinity purification (Figure 2A), but its ability to coprecipitate with RasGAP indicates that the Y1023 residue is still phosphorylated despite the mutation (Figure 2B). This suggests that recognition of negatively-charged sidechains is important for SHP2 substrate determination *in vivo* as well as *in vitro*.

Interestingly, the lost association correlated with a loss of signaling longevity in response to EGF (Figure 3A), presumably due to preserved binding of the inhibitor RasGAP. This is in agreement with the model for SHP2 mediation of HER2 signaling that was proposed previously (24). This signaling defect carried over to a defect in transformative capacity of HER2 in an anchorage-independent growth assay, further indicating a survival promoting role of the SHP2-HER2 interaction (Figure 3B).

Molecular docking was used as a tool to predict how selective binding is achieved. Specifically, electrostatic interactions of substrate acidic sidechain-containing amino acids with active site arginine 362 as well as lysine 364 (substituted to lysine and arginine in SHP1, respectively) were found to strongly mediate the binding. In addition, the difference in size of these amino acids resulted in unfavorable steric interactions when docked to SHP1 but not SHP2. We found that interactions with K364 of SHP2 conferred a significant amount of electrostatic stability, especially to the -2 position aspartate residue of the DADEpYL peptide inhibitor. We experimentally confirmed that this -2 position acidic amino acid was important for binding *in vitro,* in support of our computational docking results. The importance of the substrate's negatively-charged sidechains binding to the region containing R362 and K364 suggested that selectivity for SHP2 is derived

primarily from distinct characteristics of this region. Interestingly, the first known SHP2 inhibitor, NSC-87877, was shown to be non-selective between SHP2 and SHP1, and docking in that study revealed that the positively-charged region of the active site was not engaged by this compound at all, which may help to explain its lack of selectivity for SHP2 over SHP1 (1).

The differences in the predicted energies of polar contacts revealed special importance of sidechain interactions to the binding of acidic residue-containing peptides to SHP2, but not necessarily SHP1. Side chain interactions between the peptide's acidic residues and the active site resulted in a total energetic stabilization twice as large for SHP2 (-16.238 kcal/mol) as for SHP1 (-8.756 kcal/mol). This may explain why SHP2 is able to bind and selectively dephosphorylate EGFR pY992, while SHP1 does not. It also supports the idea that SHP1 and SHP2 have divergent active site selectivity determinants, and this selectivity is not due to trafficking by their unique SH2 domains (37).

In conclusion, we have presented data elucidating specific substrate-SHP2 intermolecular interactions that are present during binding of a substrate-derived phosphopeptide inhibitor of SHP2. Interactions with a positively-charged region of the active site that are conserved in sequence, but not structure between SHP2 and SHP1, are found to be present and appear to be critical for inhibition as determined by *in vitro* assays. This substrate-derived peptide shows substantial selectivity for SHP2 over SHP1, an improvement over currently-published inhibitors. While we do not expect this peptide to be an acceptable therapeutic agent in itself, we expect that the knowledge of selectivity determination will be useful in the development of improved small molecule inhibitors.

Figure Legends

Figure 1. a) The major phosphotyrosine sites in EGFR and HER2 were overlaid for comparison; common features to SHP2 substrate sequences were analyzed, and a substrate-derived peptide was synthesized. b) Activity of the substrate-derived peptide was assessed in competition with the fluorogenic difluoromethylumbelliferryl phosphate in increasing concentrations to arrive at an IC50 as described in Materials and Methods. The modified substrate, with the -2 position aspartate substituted, showed no activity toward SHP2.

Figure 2. a) Whole cell extracts of MCF-10A cells expressing either vector control, WT-HER2, 1023F-HER2, or 1021A-HER2 following EGF stimulation (24).

b) MCF-10A cells expressing wildtype or mutant HER2 were stimulated with EGF for 10 minutes, and lysates were subjected to immunoprecipitation with RasGAP to determine phosphorylation status of Y1023.

c) Whole-cell extracts of MCF-10A cells described in "a" were incubated overnight in the presence of GST-DM-SHP2 and glutathione-sepharose beads. Captured complexes were washed four times and then were immunoblotted for HER2.

Figure 3. a) MCF-10A cells overexpressing wildtype or mutant HER2 were stimulated with EGF (100 ng/mL) over the given time points. Lysates were subjected to SDS-PAGE and immunoblotting.

b) MCF-10A cells were subjected to an anchorage-independent growth assay as described previously (25). Briefly, 1x10^5 cells were suspended in a 0.5% agar and were allowed to grow, refreshing media every two days. Colony size was estimated as a circular area based on 10 different fields of colonies per replicate. Data are presented as mean±SEM. ***, $p<0.001$

Figure 4. a) EGFR Y992-derived peptide was docked into the SHP2 active site using Autodock4, and the binding mode is presented with SHP2 residues represented using the molecular surface model.

b) Interactions between the peptide and the SHP2 active sites. Peptide residues are labeled based on their sequence position relative to the phosphotyrosine. Polar contacts are indicated by green dots.

Figure 5. a) EGFR Y992-derived peptide was docked into the SHP1 active site using Autodock4, and the binding mode is presented with SHP1 residues represented using the molecular surface model.

b) Interactions between the peptide and the SHP1 active sites. Peptide residues are labeled based on their sequence position relative to the phosphotyrosine. Polar contacts are indicated by green dots.

Figure 1. Derivation of a substrate-derived peptide that selectively inhibits SHP2

A)

EGFR

DVVDADEY$_{992}$LIPQQG
TFLPVPEY$_{1068}$INQSVP
GSVQNPVY$_{1086}$HNQPLN
ISLDNPDY$_{1148}$QQDFFP
STAENAEY$_{1173}$LRVAPQ

HER2

DLVDAEEY$_{1023}$LVPQQG
HDPSPLQY$_{1112}$SEDPTV
TCSPQPEY$_{1139}$VNQPDV
GAVENPEY$_{1196}$LTPQGG
PAFDNLYY$_{1222}$WDQDPP
AVAENPEY$_{1248}$LGLDVP

B)

Testing wildtype peptide	
DADEpYL	Experimental Ki (μM)
SHP1	630.0
SHP2	11.97
Testing mutant peptide	
DAAEpYL	
SHP2	856.8

Figure 2. Mutation of HER2 abolishes interaction with SHP2

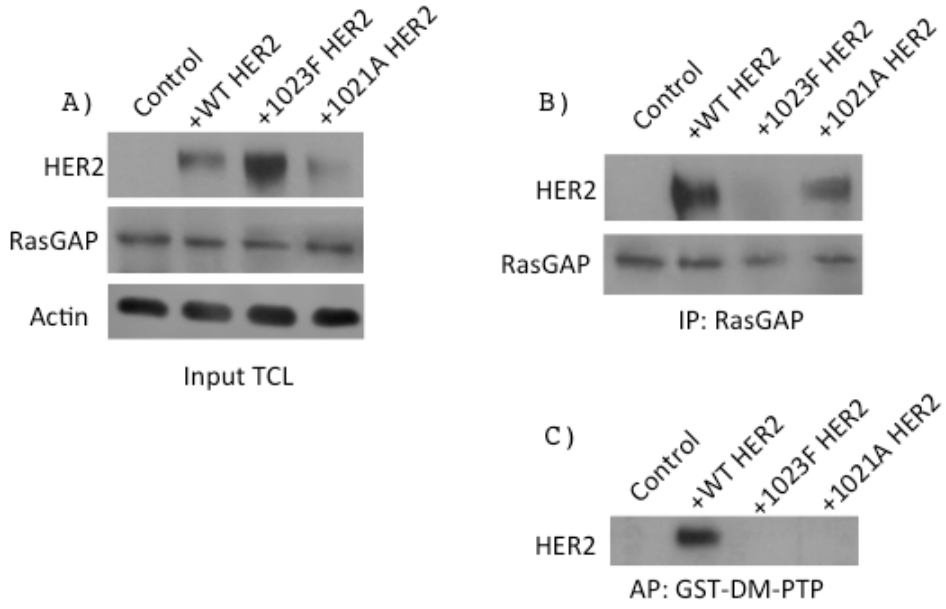

Figure 3. Mutation of HER2 results in attenuated response to EGF stimulation and inhibits transformation

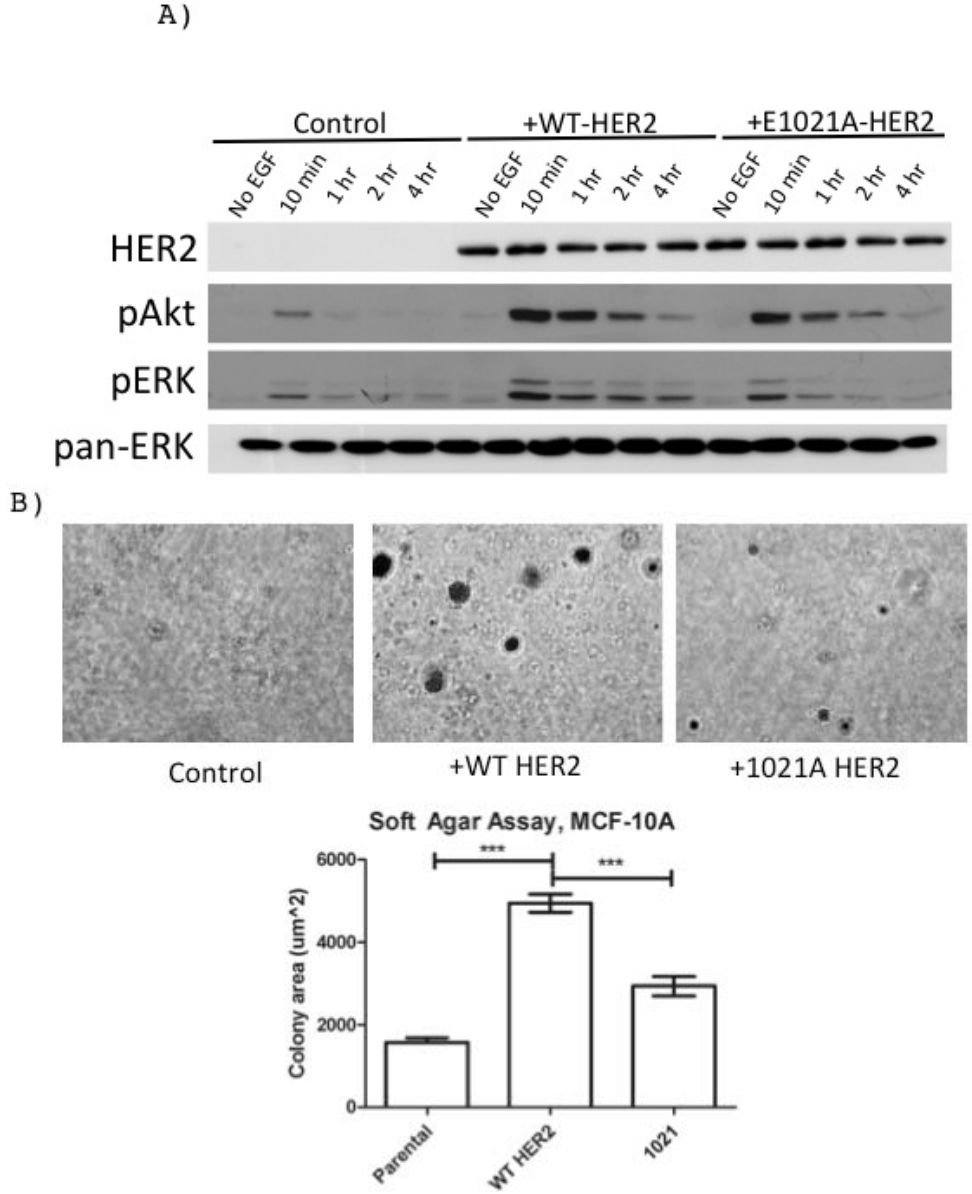

Figure 4. Predicted binding mode of substrate-derived peptide to the SHP2 active site

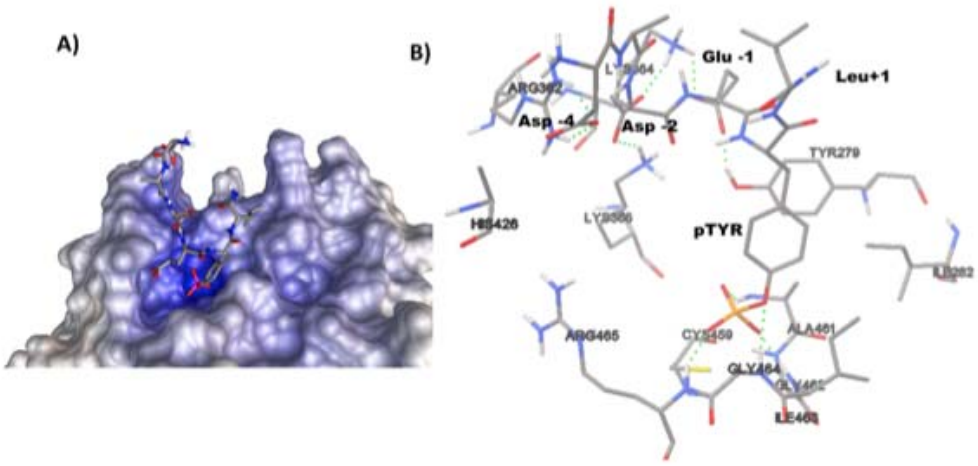

Figure 5. Predicted binding mode of substrate-derived peptide to the SHP1 active site

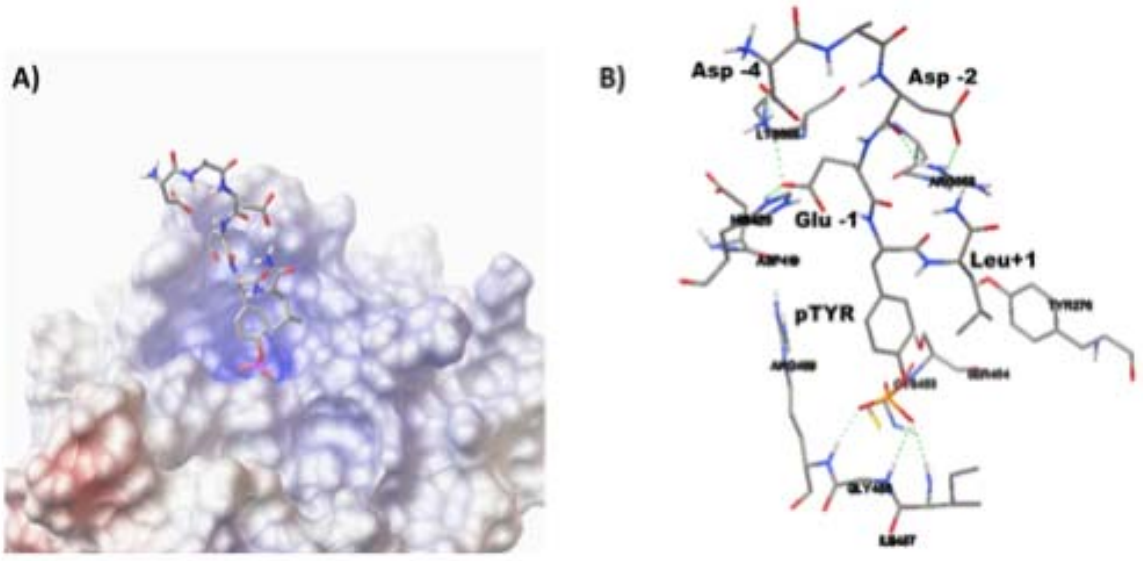

Table 1. Predicted electrostatic interactions between the substrate-derived peptide and the SHP2 active site

Peptide to SHP2	Energy*
-1 Glu to Y279	-2.903
-2 Asp toK364	-6.737
-2 Asp to K366	-0.113
-4 Asp to R362	-2.827
-4 Asp to R362	-3.653

*Energy given in kcal/mol

Table 2. Predicted electrostatic interactions between the substrate-derived peptide and the SHP1 active site

Peptide to SHP1	Energy*
-1 Glu to H420	-3.67
-1 Glu to K356	-0.301
-2 Asp to R358	-4.518
-2 Asp to R358	-0.26
-4 Asp to K356	-0.007

*Energy given in kcal/mol

REFERENCES

1. Chen, L., Sung, S. S., Yip, M. L., Lawrence, H. R., Ren, Y., Guida, W. C., Sebti, S. M., Lawrence, N. J., and Wu, J. (2006) *Molecular pharmacology* **70**, 562-562
2. Barr, A. J. *Future medicinal chemistry* **2**, 1563-1576
3. Zhou, X., and Agazie, Y. M. (2009) *The Journal of biological chemistry* **284**, 12226-12234
4. Hellmuth, K., Grosskopf, S., Lum, C. T., Wurtele, M., Roder, N., von Kries, J. P., Rosario, M., Rademann, J., and Birchmeier, W. (2008) *Proceedings of the National Academy of Sciences of the United States of America* **105**, 7275-7280
5. Morris, G. M., Goodsell, D. S., Halliday, R. S., Huey, R., Hart, W. E., Belew, R. K., and Olson, A. J. (1998) *Journal of Computational Chemistry* **19**, 1639-1662
6. Mohi, M. G., and Neel, B. G. (2007) *Current opinion in genetics & development* **17**, 23-30
7. JÃ¤rver, P., and Langel, U. (2004) *Drug discovery today* **9**, 395-402
8. Yu, Z.-H., Chen, L., Wu, L., Liu, S., Wang, L., and Zhang, Z.-Y. *Bioorganic & medicinal chemistry letters* **21**, 4238-4242
9. Zhang, X., He, Y., Liu, S., Yu, Z., Jiang, Z. X., Yang, Z., Dong, Y., Nabinger, S. C., Wu, L., Gunawan, A. M., and others. (2010) *Journal of medicinal chemistry* **53**, 2482-2493
10. Yu, Z.-H., Chen, L., Wu, L., Liu, S., Wang, L., and Zhang, Z.-Y. (2011) *Bioorganic & medicinal chemistry letters* **21**, 4238-4242
11. Hof, P., Pluskey, S., Dhe-Paganon, S., Eck, M. J., and Shoelson, S. E. (1998) *Cell* **92**, 441-450
12. Dance, M., Montagner, A., Salles, J.-P., Yart, A., and Raynal, P. (2008) *Cellular signalling* **20**, 453-459
13. Yang, W., Klaman, L. D., Chen, B., Araki, T., Harada, H., Thomas, S. M., George, E. L., and Neel, B. G. (2006) *Developmental cell* **10**, 317-327
14. Yang, Z., Li, Y., and Yin, F. (2008) *Exp. Hematol.* **36**, 1285-1296
15. Yu, D. H., Qu, C. K., Henegariu, O., Lu, X., and Feng, G. S. (1998) *The Journal of biological chemistry* **273**, 21125-21131
16. Grossmann, K., Rosario, M., Birchmeier, C., and Birchmeier, W. (2010) *Advances in Cancer Research* **106**, 53-89
17. Agazie, Y. M., Movilla, N., Ischenko, I., and Hayman, M. J. (2003) *Oncogene* **22**, 6909-6918
18. Zhou, X. D., and Agazie, Y. M. (2008) *Cell death and differentiation* **15**, 988-996
19. Chen, L., Pernazza, D., Scott, L. M., Lawrence, H. R., Ren, Y., Luo, Y., Wu, X., Sung, S.-S., Guida, W. C., Sebti, S. M., Lawrence, N. J., and Wu, J. (2010) *Biochemical pharmacology*, 1-10
20. Barr, A. J. (2010) *Future medicinal chemistry* **2**, 1563-1576
21. Shultz, L. D., Rajan, V., and Greiner, D. L. (1997) *Science* **15**, 302-307
22. (!!! INVALID CITATION !!!)
23. Ren, L., Chen, X., Luechapanichkul, R., Selner, N. G., Meyer, T. M., Wavreille, A.-S., Chan, R., Iorio, C., Zhou, X., Neel, B. G., and Pei, D. (2011) *Biochemistry* **50**, 2339-2356
24. Zhou, X., and Agazie, Y. M. (2009) *The Journal of biological chemistry* **284**, 12226-12234
25. Zhou, X. D., and Agazie, Y. M. (2008) *Cell Death Differ* **15**, 988-996
26. Version, A., Morris, G. M., Goodsell, D. S., Pique, M. E., Lindstrom, W. L., Huey, R., Hart, W. E., Halliday, S., Belew, R., and Olson, A. J. (2010), 1-49
27. Agazie, Y. M., and Hayman, M. J. (2003) *Molecular and cellular biology* **23**, 7875-7886
28. Tsutsumi, R., Takahashi, A., Azuma, T., Higashi, H., and Hatakeyama, M. (2006) *Molecular and cellular biology* **26**, 261-276
29. Ren, L., Chen, X., Luechapanichkul, R., Selner, N. G., Meyer, T. M., Wavreille, A. S., Chan, R., Iorio, C., Zhou, X., Neel, B. G., and Pei, D. (2011) *Biochemistry* **50**, 2339-2356
30. O'Reilly, A. M., and Neel, B. G. (1998) *Molecular and cellular biology* **18**, 161-177
31. Tenev, T., Keilhack, H., Tomic, S., Stoyanov, B., Stein-Gerlach, M., Lammers, R., Krivtsov, A. V., Ullrich, A., and Bohmer, F. D. (1997) *The Journal of biological chemistry* **272**, 5966-5973

32. Montalibet, J., Skorey, K. I., and Kennedy, B. P. (2005) *Methods (San Diego, Calif.)* **35**, 2-8
33. Hartman, Z. R., Schaller, M. D., and Agazie, Y. M. (2013) *Molecular cancer research : MCR* **11**, 651-664
34. Barr, A. J., Ugochukwu, E., Lee, W. H., King, O. N., Filippakopoulos, P., Alfano, I., Savitsky, P., Burgess-Brown, N. A., Muller, S., and Knapp, S. (2009) *Cell* **136**, 352-363
35. Mohi, M. G., and Neel, B. G. (2007) *Curr Opin Genet Dev* **17**, 23-30
36. Hellmuth, K., Grosskopf, S., Lum, C. T., Wurtele, M., Roder, N., von Kries, J. P., Rosario, M., Rademann, J., and Birchmeier, W. (2008) *Proceedings of the National Academy of Sciences of the United States of America* **105**, 7275-7280
37. Sweeney, M. C., Wavreille, A.-S., Park, J., Butchar, J. P., Tridandapani, S., and Pei, D. (2005) *Biochemistry* **44**, 14932-14947